Available online at www.sciencedirect.com
ScienceDirect
Journal of Sound and Vibration 319 (2009) 869–884
JOURNAL OF SOUND AND VIBRATION
www.elsevier.com/locate/jsvi

Impact load identification of composite structure using genetic algorithms

Gang Yan, Li Zhou*

College of Aerospace Engineering, Nanjing University of Aeronautics and Astronautics, Nanjing 210016, China

Received 28 August 2007; received in revised form 23 June 2008; accepted 29 June 2008
Handling Editor: L.G. Tham
Available online 27 August 2008

Abstract

For structural health monitoring of composite structure, it is important to quickly and accurately identify the impact load whenever an impact event occurs. This paper proposes a genetic algorithms (GA)-based approach for impact load identification, which can identify the impact location and reconstruct the impact force history simultaneously. In this study, impact load is represented by a set of parameters, thus the impact load identification problem in both space (impact location) and time (impact force history) domains is transformed to a parameter identification problem. A forward model characterizes the dynamic response of the structure subject to a known impact force is incorporated in the identification procedure. By minimizing the difference between the analytical responses given by the forward model and the measured ones, GA adaptively identify the impact location and force history with its global search capability. This new impact identification approach is applied to a stiffened composite panel. The stiffened composite panel is modeled as an equivalent laminate with varying properties and the forward response is obtained by using an assumed modes approach. To improve the computational efficiency, micro-GA (μGA) is employed to perform the identification task. Numerical simulation studies are conducted to demonstrate the effectiveness and applicability of the proposed method.

1. Introduction

Composite materials have been widely used in primary structurally loaded components in both commercial and military aerospace vehicles. However, composite materials are vulnerable to multi-mode damages during their manufacturing, transporting and operating process. One of the major concerns in the design of composite structure is the invisible damages caused by low-velocity impact, such as fiber breakages, matrix cracks, and delaminations, which are difficult to detect and can significantly affect the integrity of the structure. Recent advances in sensing technologies along with the developments in computation and communication have resulted in a significant interest in investigating and developing structural health monitoring (SHM) technologies that can be integrated seamlessly into the structures as a built-in diagnosis system [1]. For composites, to accurately evaluate the damage extent and the residual life of the structure, the

*Corresponding author.
E-mail address: lzhou@nuaa.edu.cn (L. Zhou).

0022-460X/$ - see front matter © 2008 Published by Elsevier Ltd.
doi:10.1016/j.jsv.2008.06.051

first task of an efficient and reliable structural health monitoring system (SHMS) is to detect and identify the impact load whenever an impact event occurs.

Generally, identifying the impact load for composite structure consists of two main aspects: identifying the impact location and reconstructing the impact force history. A number of researches have been conducted and reported for impact load identification using different approaches during the past several years [2–16]. For identifying the impact location, an effective approach is to analyze the impact-induced stress waves using joint time–frequency analysis [2,3]. By extracting the time-of-flights (TOFs) of the stress waves at different local frequencies, the impact location can be obtained by solving a set of nonlinear equations describing the relationships among impact location, group velocities and TOFs. However, this method can only be used to estimate the impact location without providing any information about the impact force history. For reconstructing impact forces, Gual and Hurlebaus [4], and Peelamedu et al. [5] proposed analytical methods to determine the relationship between the impact force and the corresponding responses with known impact location in isotropic plates. Using this relationship, the impact force history can be obtained inversely. However, it is difficult to obtain such an exact relationship for composite structures and complex structures analytically. Intelligent approaches are also employed for impact identification. Neural networks have been shown to be a promising way to identify the impact location and magnitude of impact force simultaneously [6–9]; however, it requires collecting exhausting impact data set through training tests, which may not be feasible for practical use. Up to now, the most efficient and effective reported methods that can identify both the impact location and the impact force history are based on system optimization theory [10–14]. Choi and Chang [10] developed a robust impact identification system using distributed built-in sensors. By comparing the measured sensor outputs with the estimated measurements from the system model, the impact location and force history are predicted by a smoother/filter algorithm. Tracy and Chang [11], and Seydel and Chang [12] modified this method for identifying the impact load for laminated composite plate and stiffened composite panel, respectively. Matsumoto et al. [13], and Hu et al. [14] employed finite element method to formulate the relation between the unknown force and the structural response. By comparing the numerical estimated responses and the experimental ones, optimization models are set up to solve the inverse problem by employing a modified least square method and a quadratic programming method, respectively. However, the development of these algorithms is dependent on special forms of dynamic models, such as state space model [10–12] and finite element model [13,14].

Mathematically speaking, determination of the external loads of a structure based on the sensor signals is a nonlinear inverse problem. As a global optimization technique, genetic algorithms (GA) is normally taken as a method of choice for such problems, and can be employed for impact load identification. Coverley and Staszewski [15], and Haywood et al. [16] proposed a triangulation procedure incorporating a GA to localize the impact location, demonstrating the promising potential of GA in impact load identification. However, their work only considered the identification of impact location, how to identify the impact force history using GA is not concerned.

The aim of this work is to provide a GA-based approach to identify the impact location and reconstruct the impact force history simultaneously. In particular, a case of impact identification for stiffened composite panel is presented. Micro-GA (μGA) is employed to perform the identification task with its global search capability and high computational efficacy. The paper is structured as follows. Section 2 describes the impact load identification strategy. In Section 3, a brief introduction of μGA and its application in this study is presented. The forward model for stiffened composite panel using equivalent plate analysis and assumed modes method is described in Section 4. Numerical simulation study is performed in Section 5 to verify the proposed impact load identification strategy. Finally, concluding remarks are given in Section 6.

2. Impact load identification strategy

Fig. 1 illustrates the proposed impact load identification strategy in this study. The impact load identification problem is formulated as an optimization problem, thus the nonlinear inverse identification problem which is non-unique and instable is transformed to a forward problem. The first step of this identification strategy is to represent the impact load with a set of proper parameters. This parameterization allows the impact identification problem, especially the reconstruction of impact force history, to be more

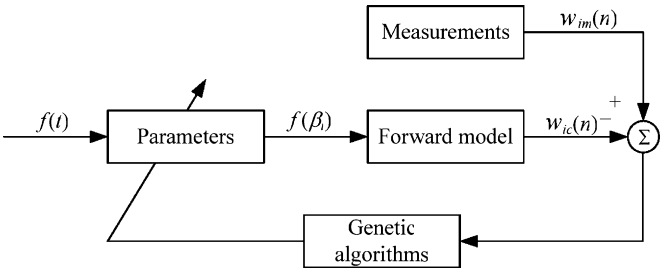

Fig. 1. A general impact load identification strategy.

simple and tractable, since identifying several unknown parameters is much easier than directly reconstructing the values of impact force at the many discrete time points in the time domain [14]. In another way, it enables identifying the unknown impact location in space domain and the parameters portraying the impact force history in time domain simultaneously within a single algorithm. Then, combining with a forward model, which characterizes the dynamic response of the structure subject to a known impact force, the unknown parameters depicting the impact location and impact force history can be identified by minimizing the difference between the computed analytical responses and the actually measured responses. There is no limitation for the forward impact response model. It may be a physical model, such as finite element model, or a surrogate model. However, for real application, the forward model should be accurate and fast, increasing the computational efficacy of the identification algorithm.

In the proposed identification strategy, a problem arising from the identification process is that the resulting optimization problem is nonlinear and multi-modal especially for complex structures. Gradient functions or other additional differential information, which is required by traditional optimization approaches, may be difficult and time-consuming to calculate or even cannot be obtained depending on the model chosen, thus GA are employed in this impact load identification strategy. Other intelligent algorithms with global search capability, such as simulated annealing (SA), also meet the requirement. From Fig. 1, it can be clearly seen that each of the steps can be incorporated with different methods, providing a general and flexible approach for complex composite structures. In the following, a case of impact identification for stiffened composite panel is presented to demonstrate the effectiveness and applicability of this proposed impact load identification strategy. A special form of GA, μGA, is employed in this study to perform the optimization work.

The basic idea of this identification strategy is to parameterize the impact load. A general method for approximating a force history in time domain is to use a series of smooth base functions $\varphi_i(t)$, such as trigonometric polynomial or Chebyshev polynomial [14], thus the impact force $f(t)$ can be written as

$$f(t) = f(\beta_i) = \sum_{i=1}^{N_f} \beta_i \varphi_i(t), \quad t \in [0, T] \tag{1}$$

where the coefficients β_i of each base function constitute the unknown parameters to be identified. A recent study conducted by Hu et al. [14] shows that this parameterizing approach can approximate the impact force history very well; however, the disadvantage is that it may need too many numbers of base functions to obtain converged results, about 30–40 in Ref. [14], leading to a large search space and slow convergence rate. A simple but effective impact force representation method with a few unknown parameters is proposed in this study.

Observing the experimentally measured impact load, researches have shown that a general impact force history can be represented as a half-sine pulse shape [5,10]. In this study, the impact force history is approximately considered as a combination of two 1/4 cycle-sine pulses, while the loading frequency and unloading frequency are different, as illustrated in Fig. 2. Therefore, five parameters are used to depict such a general impact load, namely the impact location (x_{impact}, y_{impact}), the magnitude of the impact force $f_{\max}$, the loading frequency ω_{load} and the unloading frequency ω_{unload} of the impact force. For simplicity, only impact perpendicular to the structure is considered, and the material degradation caused by impact is not considered.

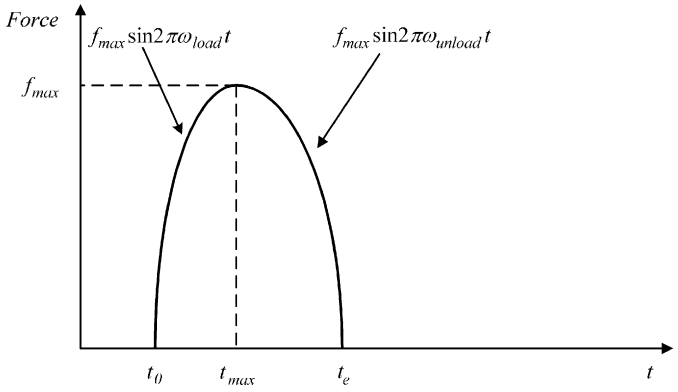

Fig. 2. The general representation of impact force history.

After the unknown parameters to be identified are defined, the impact load identification is formulated as an optimization problem to be solved. In this study, for demonstrating the effectiveness of the proposed algorithm, the transverse displacement response w of the structure under impact is taken as the measurement. However, in real application with built-in sensors, the strain responses are usually taken as the measured responses for convenience. The difference between the theoretical outputs of the forward model and the measurements

$$\begin{aligned}&\mathrm{Err}(x_{\mathrm{impact}}, y_{\mathrm{impact}}, f_{\max}, \omega_{\mathrm{load}}, \omega_{\mathrm{unload}})\\&= \sum_{i=1}^{N_p}\left(\sum_{n=1}^{N_s}\left|w_{\mathrm{im}}(n) - w_{\mathrm{ic}}(x_{\mathrm{impact}}, y_{\mathrm{impact}}, f_{\max}, \omega_{\mathrm{load}}, \omega_{\mathrm{unload}}, n)\right|^2\right)^{1/2}\end{aligned} \tag{2}$$

is used as the objective function to be minimized during the optimization process. In Eq. (2), N_s is the number of discrete sampling points in the time domain, and N_p is the number of sensors used for recording responses for identification.

Since μGA is employed in this study as the intelligent optimization algorithm to perform the identification work, a fitness value is designated for the genetic operators to perform evolution in μGA. This fitness value reflects the performance of the solution searched, namely the desired objective value. In this study, the fitness function is defined as

$$\mathrm{Fit}(x_{\mathrm{impact}}, y_{\mathrm{impact}}, f_{\max}, \omega_{\mathrm{load}}, \omega_{\mathrm{unload}}) = \frac{1}{c_1\mathrm{Err}(x_{\mathrm{impact}}, y_{\mathrm{impact}}, f_{\max}, \omega_{\mathrm{load}}, \omega_{\mathrm{unload}}) + c_2} \tag{3}$$

where c_1 and c_2 are proper constants to make sure the fitness value is a positive finite number, and *Err* is the objective value defined in Eq. (2).

3. Micro-genetic algorithm

As a powerful computational search and optimization tool, GA is an adaptive heuristic search algorithm based on the evolutionary ideas of natural selection and genetics [17,18]. GA differs from conventional mathematical optimization methods in two ways. First, GA does not operate directly on the parameters to be searched, but on a coded representation of the parameters. Analogous to genes in genetics, GA represents the parameters in a given problem by encoding them in a string, called chromosome. Second, instead of finding the optimum from a single point in traditional optimization methods, GA works on a set of points, that is, a population of chromosomes, at a time. This implicit parallelism makes GA capable of searching the solution in a global manner. GA requires only the specification of an objective function or a fitness function to search the optimal point, rather than gradient functions or other additional differential information, which are always difficult and time-consuming to calculate or even cannot be obtained in highly-nonlinear and

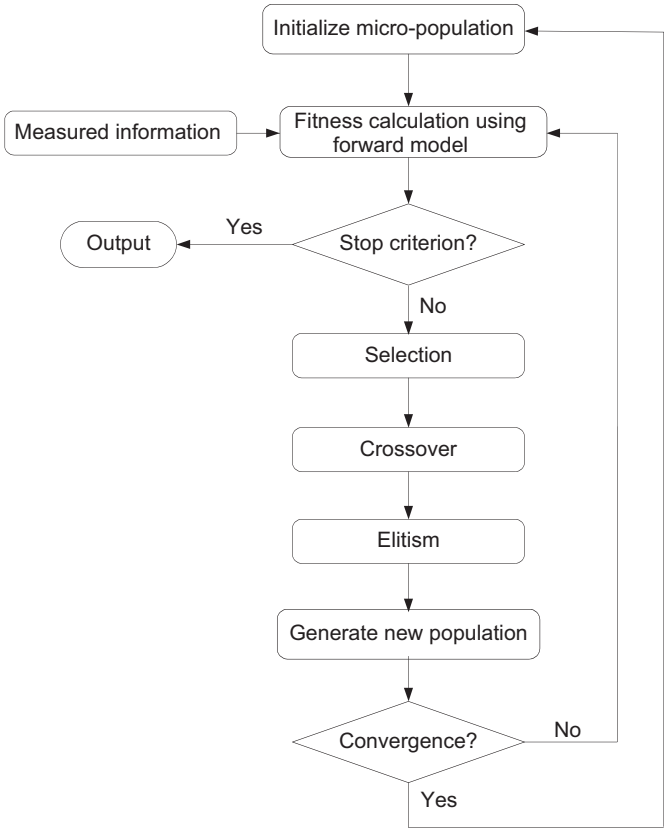

Fig. 3. Flowchart of μGA-based impact load identification.

multi-modal problems. During the search process, GA uses operations of selection (reproduction), crossover, and mutation on a population of chromosomes to perform evolution toward global (or near global) optimum.

However, a serious limitation of traditional GA is the time penalty involved in evaluating the fitness functions for large populations, particularly in complex problems. To improve computational efficacy, μGA is employed to accelerate convergence in this study. In comparison with traditional GA, GA with small populations is called μGA [19]. By restarting the small population with sufficient number of times, μGA can successfully avoid premature convergence and demonstrate faster convergence to the near optimal region for nonlinear multi-modal problems [20]. Fig. 3 shows the flowchart of μGA for impact identification in this study. As illustrated in the figure, the optimization process for impact load identification can be stepped as follows:

(1) Encode the parameters of the impact load into chromosomes for GA operation. In this study, the most commonly used binary bit-string encoding is adopted to encode the parameters to be identified. Each parameter is encoded into a ten-bit string, leading to a 50-bit-long chromosome that represents a possible solution containing the unknown parameters (x_{impact}, y_{impact}, $f_{\max}$, ω_{load}, ω_{unload}).
(2) Randomly generate the initial population with N_c ($N_c = 5$–8) chromosomes for the first time, or N_c-1 chromosomes with the best individual of the previous generation during other restarting process, to form a micro-population. In this study, N_c is selected as 6.
(3) Decode the chromosomes and substitute them into the forward model to compute the analytical responses for calculating fitness values defined in Eq. (3). The individual with highest fitness in current generation is directly selected as the parent of the next population. This elitism mechanism keeps the best genetic information in the population and can rapidly increase the performance of GA.

(4) Perform GA operations, i.e. selection, crossover to the other N_c-1 chromosomes toward global (or near global) optimum. In this study, tournament selection and uniform crossover are implemented to the micro-population. Since new individuals are continuously introduced by the restarting mechanism to keep variability of the population, another operation in traditional GA, i.e., mutation, is not performed.
(5) Determine whether the micro-population is convergent. Since small populations, the inner loop converges rapidly as compared to the traditional GA. A restart process regenerating a new population is employed to introduce diversity once the difference between the genes of the best chromosome and other ones in the population is below 5%, which is the convergence criterion defined by Carroll [20].
(6) Repeat the steps of (2)–(5), until the stop criterion reaches. Output the individual with the highest fitness value in the final generation as the solution of the problem.

4. Forward model of stiffened composite panel

Generally speaking, the identification approach proposed in Fig. 1 can be categorized as a model-dependent method, and repeated running the forward model is required. Model-based methods usually undertake analysis by implementing finite element analysis. However, finite element method expends too much computational time for iterative running during the identification process, especially for complex structures. An effective and efficient modeling approach for complex structure is to consider it as an equivalent plate using the assumed modes method, which is a Rayleigh-Ritz solution in terms of energy with assumed shape functions that satisfy the geometric boundary conditions [21–23]. Based on the work of Refs. [21–23], Seydel and Chang [12] developed a forward impact model for stiffened composite panel with the advantages of few degrees of freedom, accuracy of modeling and generalization to handle various arrangements of stiffeners and boundary conditions. This modeling approach is adopted in this study for forward impact response of stiffened composite panels, and it is presented in this section for completeness.

The basic assumption of this approach is that the stiffened composite panel could be represented as a plate with varying properties [12,21–23]. The whole stiffened panel is divided into three different regions: bay, flange and rib. Each of the regions is assumed to have constant plate property as illustrated in Fig. 4. For calculation of mass and stiffness matrices assuming all sections are plate-like, the effective plate properties should be formulated first.

For the bay and flange, the plate properties D_{ij} for modeling structural dynamics can be formulated as

$$D_{ij}^{\text{bay}} = \frac{1}{3}\sum_{k=1}^{N_{\text{plys}}} Q_{ij}^{k}\left(z_k^3 - z_{k-1}^3\right) \tag{4}$$

$$D_{ij}^{\text{flange}} = \frac{1}{3}\sum_{k=1}^{N_{\text{plys}}} Q_{ij}^{k}\left(z_k^3 - z_{k-1}^3\right) \tag{5}$$

using standard lamination theory [24], where Q_{ij} is the in-plane stiffness for ply k, and z_k is the distance from the neutral axis. The neural axis is assumed to be the middle of the plate for that region.

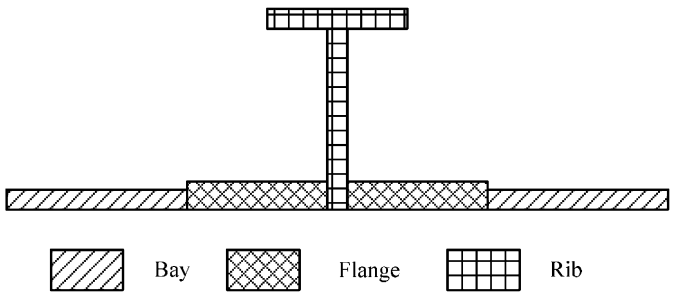

Fig. 4. Constant property sections of the stiffened panel [12].

For the rib sections, the beam properties along the rib's principal axis, the bending stiffness EI and the torsional stiffness GJ are converted to the effective plate properties as

$$D_{11} = \frac{EI}{d} \tag{6}$$

$$D_{66} = \frac{GJ}{4d} \tag{7}$$

$$\rho h = \frac{\rho A}{d} \tag{8}$$

where d is the effective width, and A is the rib cross-sectional area.

With all of the effective plate properties calculated, the structural dynamic model can be formulated. Based on classical laminate theory [24], the governing equation for a composite plate with a symmetric lay-up under a point impact is

$$\begin{aligned} f(t)\delta(x - x_{\text{impact}}, y - y_{\text{impact}}) = \rho h \frac{\partial^2 w}{\partial t^2} &+ \frac{\partial^2}{\partial x^2}\left(D_{11}\frac{\partial^2 w}{\partial x^2} + D_{12}\frac{\partial^2 w}{\partial y^2} + 2D_{16}\frac{\partial^2 w}{\partial x\,\partial y}\right) \\ &+ \frac{\partial^2}{\partial y^2}\left(D_{12}\frac{\partial^2 w}{\partial x^2} + D_{22}\frac{\partial^2 w}{\partial y^2} + 2D_{26}\frac{\partial^2 w}{\partial x\,\partial y}\right) \\ &+ 2\frac{\partial^2}{\partial x\,\partial y}\left(D_{16}\frac{\partial^2 w}{\partial x^2} + D_{26}\frac{\partial^2 w}{\partial y^2} + 2D_{66}\frac{\partial^2 w}{\partial x\,\partial y}\right) \end{aligned} \tag{9}$$

where $f(t)$ is the impact force, $(x_{\text{impact}}, y_{\text{impact}})$ is the impact location, D_{ij} is the bending stiffness matrix, w is the transverse displacement, ρh is the mass per unit area of the laminate.

In the assumed modes method, to eliminate the spatial dependence, each term of Eq. (9) is multiplied by a vector of shape functions, $\phi(x,y)$ and integrated over the dimensions X by Y in x-and y-direction, respectively. By choosing ϕ to satisfy different boundary conditions, Eq. (9) can be simplified as

$$f(t)\phi(x_{\text{impact}}, y_{\text{impact}}) = \int_0^X \int_0^Y \left\{ \begin{aligned} &\rho h \frac{\partial^2 w}{\partial t^2}\phi \\ &+\left(D_{11}\frac{\partial^2 w}{\partial x^2} + D_{12}\frac{\partial^2 w}{\partial y^2} + 2D_{16}\frac{\partial^2 w}{\partial x\,\partial y}\right)\frac{\partial^2 \phi}{\partial x^2} \\ &+\left(D_{12}\frac{\partial^2 w}{\partial x^2} + D_{22}\frac{\partial^2 w}{\partial y^2} + 2D_{26}\frac{\partial^2 w}{\partial x\,\partial y}\right)\frac{\partial^2 \phi}{\partial y^2} \\ &+2\left(D_{16}\frac{\partial^2 w}{\partial x^2} + D_{26}\frac{\partial^2 w}{\partial y^2} + 2D_{66}\frac{\partial^2 w}{\partial x\,\partial y}\right)\frac{\partial^2 \phi}{\partial x\,\partial y} \end{aligned} \right\} \mathrm{d}y\,\mathrm{d}x \tag{10}$$

The details for selection of shape function can be found in Refs. [25,26].

Approximating the displacement w by N_m terms of ϕ

$$w(x, y, t) \cong \sum_{i=1}^{N_m} \bar{w}_i(t)\phi_i(x, y) \tag{11}$$

the equation of motion can be written in the general form

$$\mathbf{M}\frac{\partial^2 \bar{\mathbf{w}}}{\partial t^2} + \mathbf{K}\,\bar{\mathbf{w}} = \mathbf{F}f(t) \tag{12}$$

where $\bar{\mathbf{w}}$ is the generalized displacement vector and $\bar{\mathbf{w}} = [\bar{w}_1 \quad \bar{w}_2 \quad \cdots \quad \bar{w}_{N_m}]^{\mathrm{T}}$; $\mathbf{F}$, $\mathbf{M}$, and $\mathbf{K}$ are the generalized force, mass and stiffness matrices, respectively:

$$F_i = \phi_i(x_{\text{impact}}, y_{\text{impact}}) \tag{13}$$

$$M_{ij} = \sum_{k=1}^{N_{\text{regions}}} \rho h^k \int_{x_{1k}}^{x_{2k}} \int_{y_{1k}}^{y_{2k}} \phi_i \phi_j \, \mathrm{d}y \, \mathrm{d}x \tag{14}$$

$$K_{ij} = \sum_{k=1}^{N_{\text{regions}}} \int_{x_{1k}}^{x_{2k}} \int_{y_{1k}}^{y_{2k}} \left\{ \begin{array}{l} D_{11}^k \dfrac{\partial^2 \phi_i}{\partial x^2} \dfrac{\partial^2 \phi_j}{\partial x^2} + D_{12}^k \left(\dfrac{\partial^2 \phi_i}{\partial y^2} \dfrac{\partial^2 \phi_j}{\partial x^2} + \dfrac{\partial^2 \phi_i}{\partial x^2} \dfrac{\partial^2 \phi_j}{\partial y^2} \right) \\ \quad + D_{16}^k \left(\dfrac{\partial^2 \phi_i}{\partial x \, \partial y} \dfrac{\partial^2 \phi_j}{\partial x^2} + 2 \dfrac{\partial^2 \phi_i}{\partial x^2} \dfrac{\partial^2 \phi_j}{\partial x \, \partial y} \right) + D_{22}^k \dfrac{\partial^2 \phi_i}{\partial y^2} \dfrac{\partial^2 \phi_j}{\partial y^2} \\ \quad \times D_{26}^k \left(2 \dfrac{\partial^2 \phi_i}{\partial x \, \partial y} \dfrac{\partial^2 \phi_j}{\partial y^2} + 2 \dfrac{\partial^2 \phi_i}{\partial x \, \partial y} \dfrac{\partial^2 \phi_j}{\partial y^2} \right) + 4 D_{66}^k \dfrac{\partial^2 \phi_i}{\partial x \, \partial y} \dfrac{\partial^2 \phi_j}{\partial x \, \partial y} \end{array} \right\} \mathrm{d}y \, \mathrm{d}x \tag{15}$$

In Eqs. (14) and (15), the contributions from the various regions are added together, x_1, x_2 and y_1, y_2 are the integral limits of region k.

Defining the state vector $\mathbf{z} = [\,\bar{\mathbf{w}} \quad \dot{\bar{\mathbf{w}}}\,]^{\mathrm{T}}$, Eq. (12) can be formulated in the state space form:

$$\dot{\mathbf{z}} = \mathbf{A}\,\mathbf{z} + \mathbf{B} f(t) \tag{16}$$

where

$$\mathbf{A} = \begin{bmatrix} \mathbf{0} & \mathbf{I} \\ -\mathbf{M}^{-1}\mathbf{K} & \mathbf{0} \end{bmatrix}, \quad \mathbf{B} = \begin{bmatrix} \mathbf{0} \\ \mathbf{M}^{-1}\mathbf{F} \end{bmatrix}$$

The impact response can be written in the output equation form:

$$\mathbf{y} = \mathbf{C}\,\mathbf{z} \tag{17}$$

where the output matrix $\mathbf{C}$ is dependent on the response $\mathbf{y}$.

Assuming zero-order hold for the input, the system is converted from continuous form to discrete time for numerical calculations:

$$\mathbf{z}(n+1) = \mathbf{\Phi}\,\mathbf{z}(n) + \mathbf{\Gamma} f(n) \tag{18}$$

$$\mathbf{y}(n) = \mathbf{C}\,\mathbf{z}(n) \tag{19}$$

where $\mathbf{\Phi} = \exp(\mathbf{A}T_s)$, $\mathbf{\Gamma} = \int_0^{T_s} \exp(\mathbf{A}t)\mathrm{d}t\mathbf{B}$, T_s is the discrete sampling time.

5. Numerical studies

5.1. Verification of forward model

To demonstrate and verify the proposed impact load identification strategy, numerical studies are conducted in this section. First, the widely used finite element software MSC.Nastran is used to verify the forward impact model of stiffened composite panel as described in Section 4. A square stiffened composite panel with dimensions of 600 mm × 600 mm shown in Fig. 5 is considered. Three parallel I-beam stiffeners run the length of the panel in the x-direction. The distance between neighboring stiffeners is 150 mm. The details about the locations of the ply groups are shown in Fig. 5. The layups of the different ply groups contain plies stacked according to the sequences given in Table 1, and consist of T300 graphite fibers and a QY8911 epoxy matrix. The thickness of each lamina is 0.125 mm. The material properties of T300/QY8911 are presented in Table 2. In the finite element model, the bay, flange and rib of the stiffened composite panel are modeled by totally 2880 quad shell elements. The stiffeners are considered as ideally bonded to the plate. All of the four edges of the panel are clamped and the origin of the coordinate system is set at the left-bottom corner as shown in Fig. 5. A set of sensors, numbered from Sensor 1 to Sensor 12 and spacing uniformly on the surface of the panel, are employed to measure the displacement responses under the impact. For reference, Sensor 1 is set at (150 mm, 75 mm), and the spacing of the sensors in x- and y-direction is 150 mm.

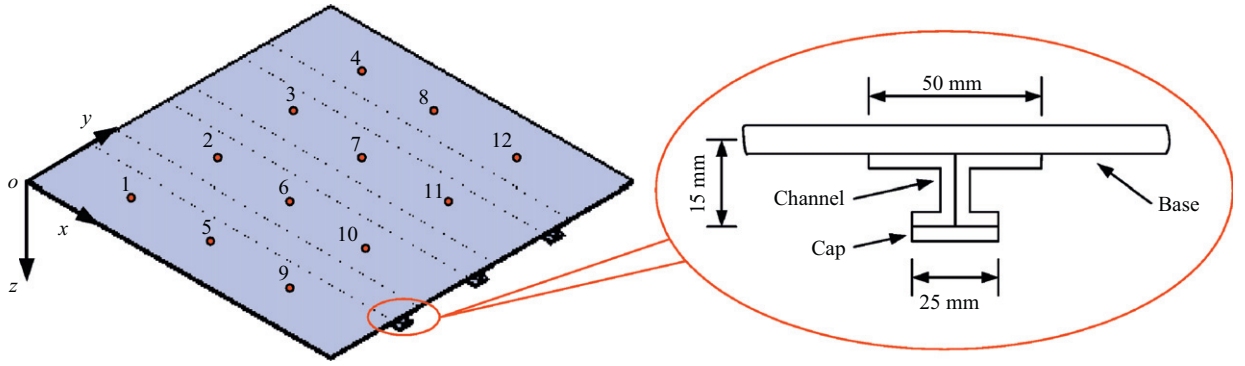

Fig. 5. Stiffened composite panel and sensor placement in numerical study.

Table 1
Group layups for the stiffened composite panel

Location	Layup
Cap	$[45/90_2/0/-45/0_3/-45/0_2/45/0]_s$
Channel	$[45/90_2/0/-45/0_3/-45/0_2/45/0]_s$
Base	$[45/90/-45_2/0/45/0/-45_2/0/45/90/45/0]_s$

Table 2
Material properties of T300/QY8911

E_1 (GPa)	E_2 (GPa)	G_{12} (GPa)	v_{12}	ρ (kg/m^3)
135	8.8	4.47	0.3	1560

For comparison of the forward model of the stiffened composite panel used in this study with finite element model, dynamic responses under impact load are examined. Assuming that a half-sine pulse shape impact load with magnitude of 1000 N and frequency of 100 Hz is acted on the center of the panel, where the coordinates are (300 mm, 300 mm). The sensors monitor and record the dynamic responses once the impact event occurs. Fig. 6 shows a comparison of impact responses by the forward model and those by finite element method at three sensor locations. The outputs of the forward model agree very well with the finite element results, verifying the equivalent laminate theory and assumed modes method for stiffened composite panel. However, the computational efficiency of the forward model is much better than the finite element model. After the generalized force, mass and stiffness matrices in Eqs. (13)–(15) are prepared, it takes less than 0.05 s for the forward model in Eqs. (16)–(19) to calculate the impact responses for 10 ms with a time step of 0.1 ms in a PC with Intel P4 3.0 GHz CPU and 1 GB memory. This is about two orders faster than the finite element model in the same PC. Therefore, the forward model presented in Section 4 is adopted in this study for modeling dynamic responses of stiffened composite panels subject to impact load and repeated running during the impact identification process.

5.2. *Results of impact load identification*

One experimental measured impact force history with maximum force of 615 N is obtained from Fig. 25 of Ref. [12] is employed in this numerical study to verify the proposed impact identification strategy. This impact force is applied on different parts of the stiffened composite panel. The impact locations considered in this numerical study for rib, flange and bay are (300 mm, 300 mm), (225 mm, 287.5 mm) and (225 mm, 225 mm), respectively. To consider the effect of model deviation, in this simulation stage, the assumed measured

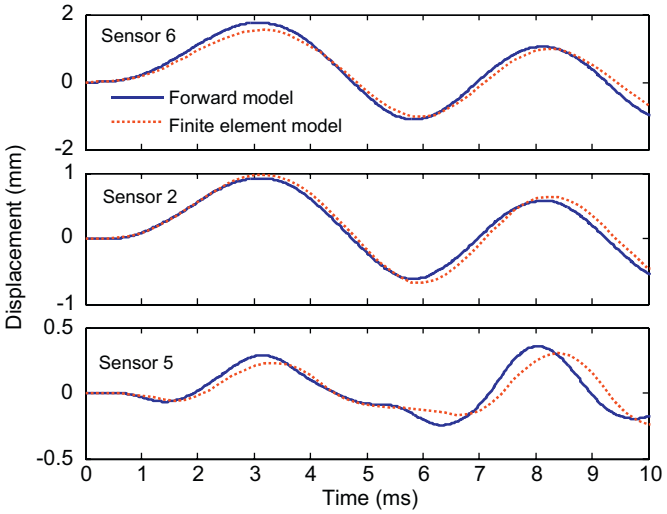

Fig. 6. Comparison of impact responses by forward model and finite element model.

displacement responses are obtained by inputting the impact loads to the finite element software MSC.Nastran. Random white noises with noise level $R = 5\%$ are added to the finite element responses. In this study, the noise level is defined as $R_i = \sigma_i/\max|w_i(t)|$ in which σ_i is the root mean square (RMS) value of the noise associated with the measurement $w_i(t)$. With these simulated responses, the proposed μGA-based impact identification strategy is implemented to obtain the parameters about the impact load.

One appealing advantage of GA is that it can be adaptively convergent to the optimum in a large search space without setting suitable initial search points which is a crucial requirement for traditional mathematical optimization approaches. In this study, the search ranges are set as following: 0–600 mm for the impact location, 0–2000 N for the magnitude of impact force, and 250–1500 Hz for the loading and unloading frequencies, respectively. Fig. 7 shows the evolution process and results for identifying the impact load using μGA when the impact load is applied on the rib at (300 mm, 300 mm). From Fig. 7(a), it can be seen that during the GA evolution, since new individuals are continuously introduced, the average fitness value of the micro-population changes rapidly, however, the best individual is keeping better and better, demonstrating the effectiveness of μGA. Fig. 7(b)–(d) shows the identification results of the impact location, magnitude of the impact force, and the loading and unloading frequencies for describing the impact force, respectively. The identified impact location is (298 mm, 307 mm), and the identified magnitude of impact force is 625.6 N, closing to the actual ones. Fig. 7(e) illustrates a comparison of the reconstructed impact force history with the measured impact force history. Though the identified force just approximately represents the real impact force, the duration and magnitude matches the measured one quite well. Fig. 7(f) shows a comparison of the displacement responses under the identified impact force acting on the identified impact location and the measured displacement responses.

Fig. 8 shows the evolution process and a comparison of the identified results using μGA with the actual impact load when the impact force is applied on the flange at (225 mm, 287.5 mm). The identified impact location is (224 mm, 297 mm), and the identified magnitude of impact force is 594.3 N. Fig. 9 shows the evolution process and a comparison of the identified results using μGA with the actual impact load when the impact force is applied on the bay at (225 mm, 225 mm). The identified impact location is (225 mm, 224 mm), and the identified magnitude of impact force is 582.6 N. From Figs. 7–9, it can be clearly seen that the identified results agree the actual values very well, demonstrating the effectiveness of the proposed impact load identification strategy.

For composite, the impact damage patterns and damage extents are tightly related to the maximum impact force and impact energy. Thus, besides the identified results illustrated in Figs. 7–9, the maximum forces and impact energies of the identified and measured impact force history are presented for comparison.

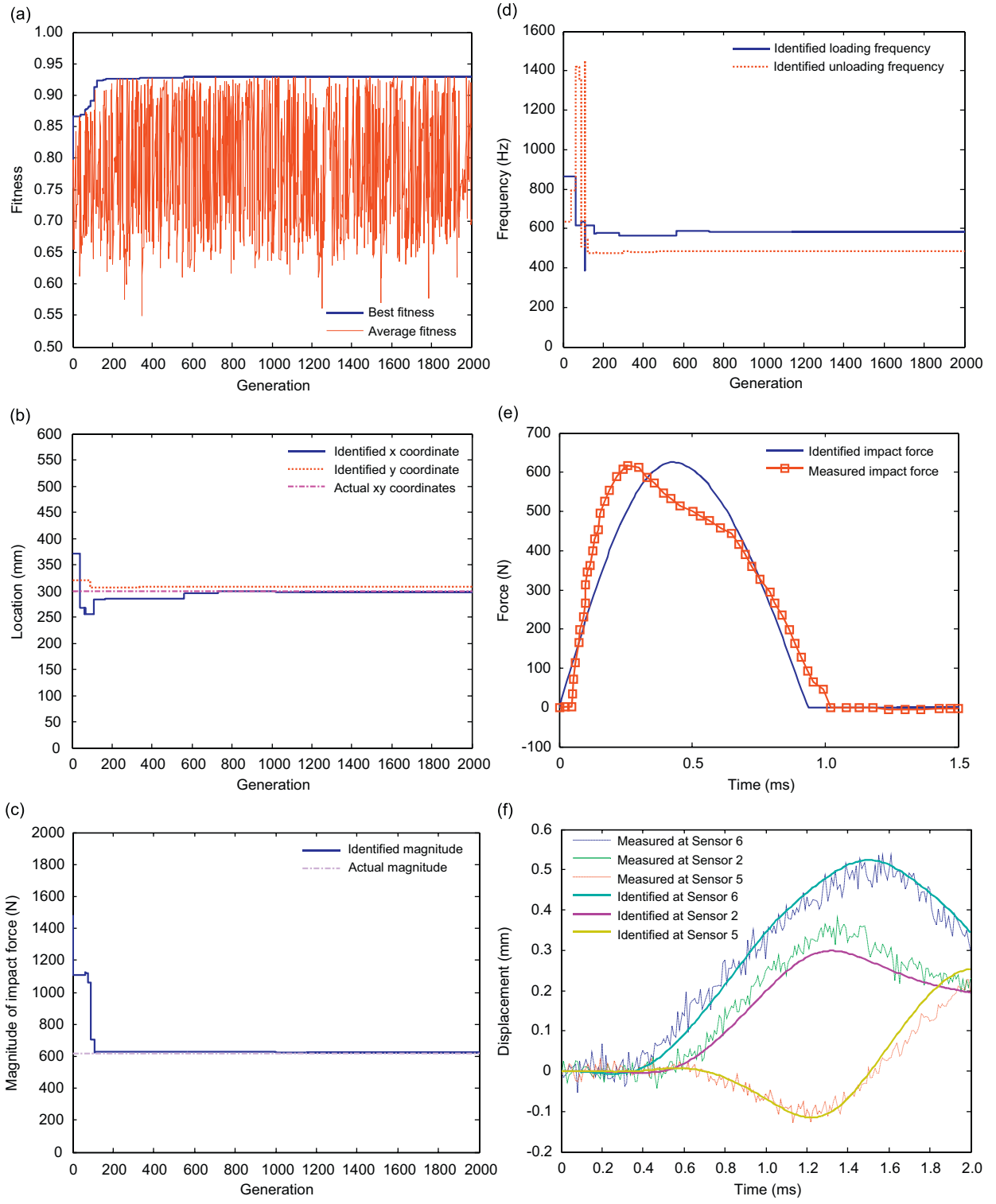

Fig. 7. Identified results by μGA when impact on rib. (a) Evolution of fitness value, (b) identified impact location, (c) identified magnitude of impact force, (d) identified loading and unloading frequencies, (e) comparison of identified and actual impact force histories and (f) comparison of identified and measured impact responses.

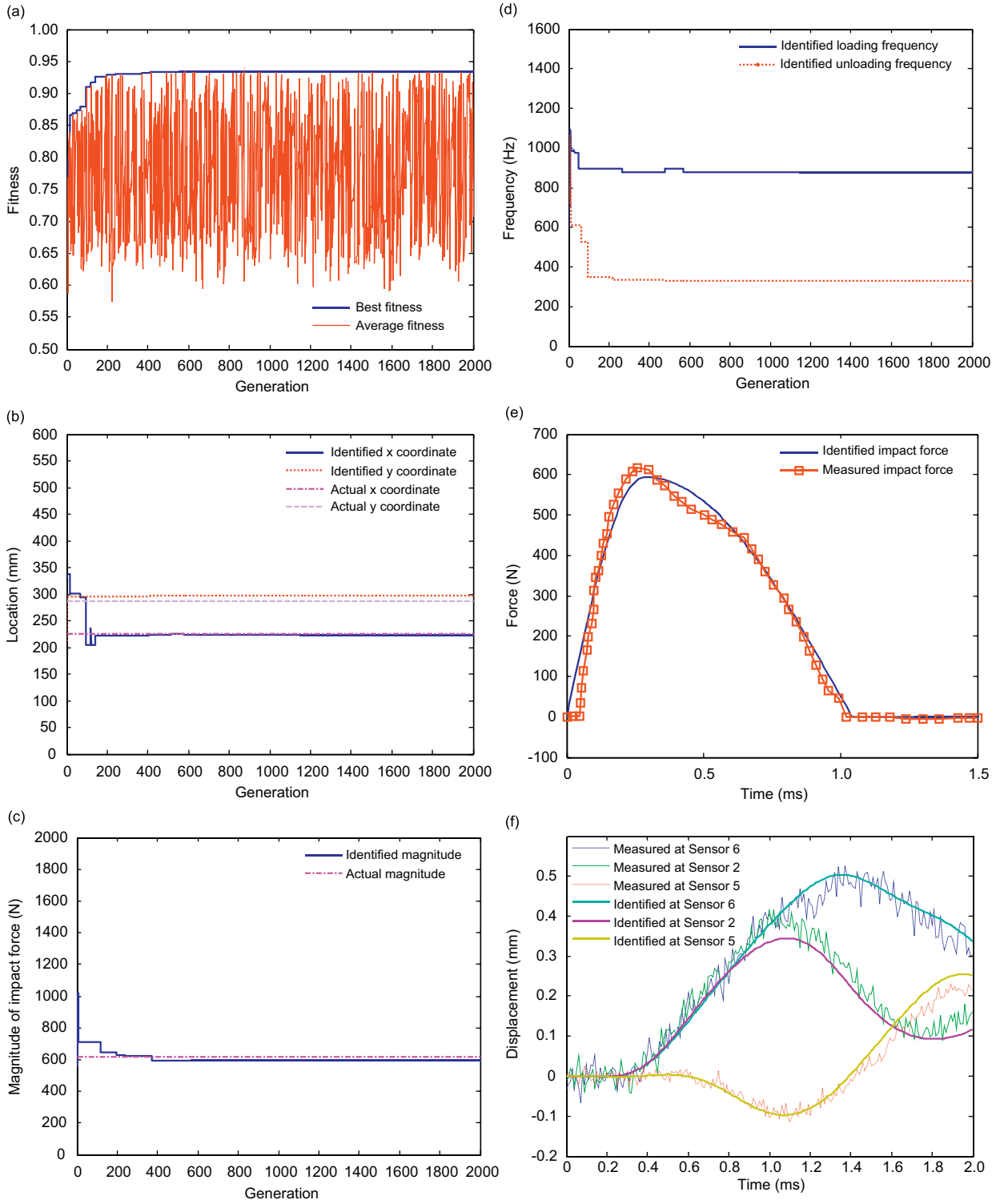

Fig. 8. Identified results by μGA when impact on flange. (a) Evolution of fitness value, (b) identified impact location, (c) identified magnitude of impact force, (d) identified loading and unloading frequencies, (e) comparison of identified and actual impact force histories and (f) comparison of identified and measured impact responses.

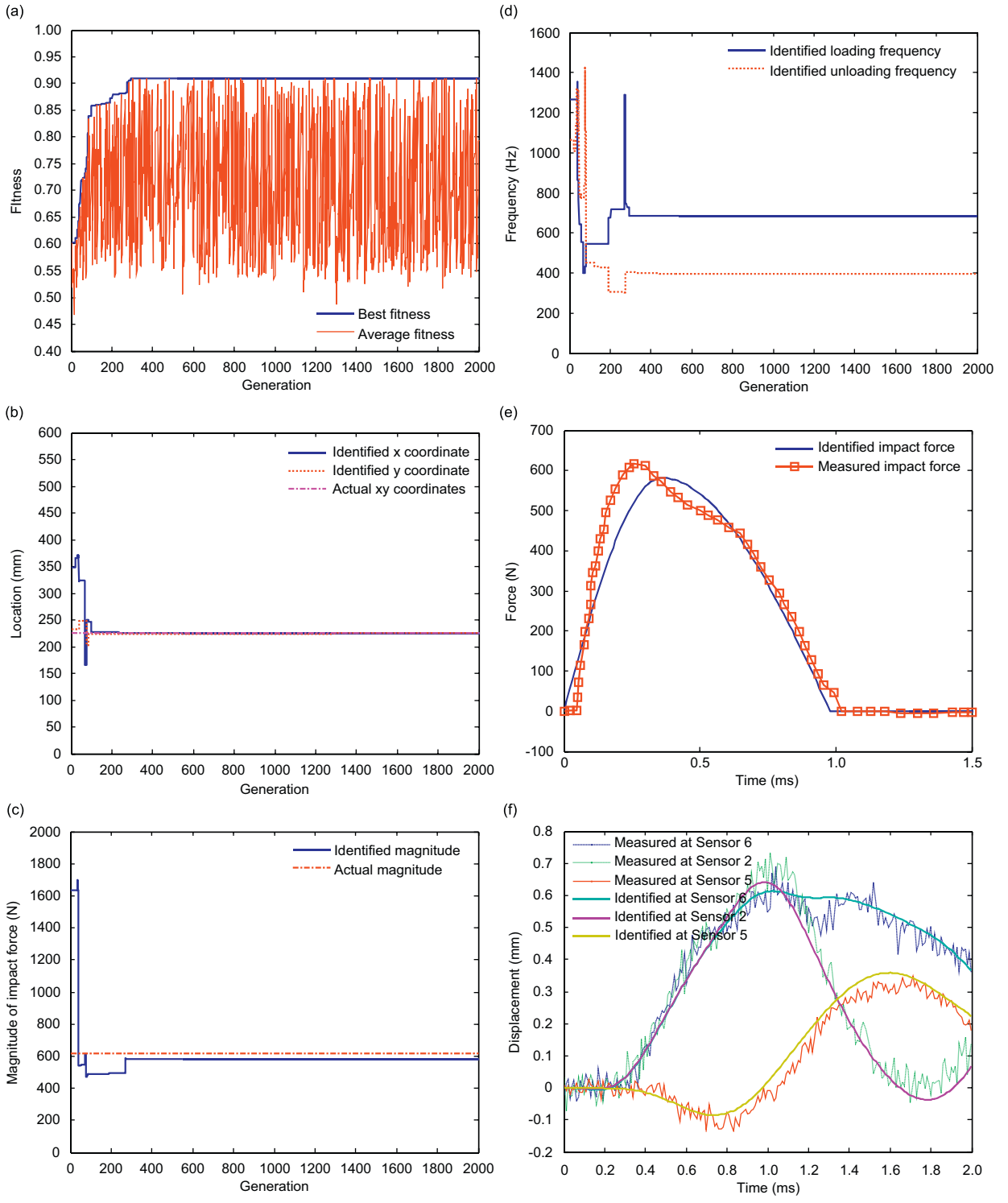

Fig. 9. Identified results by μGA when impact on bay. (a) Evolution of fitness value, (b) identified impact location, (c) identified magnitude of impact force, (d) identified loading and unloading frequencies, (e) comparison of identified and actual impact force histories and (f) comparison of identified and measured impact responses.

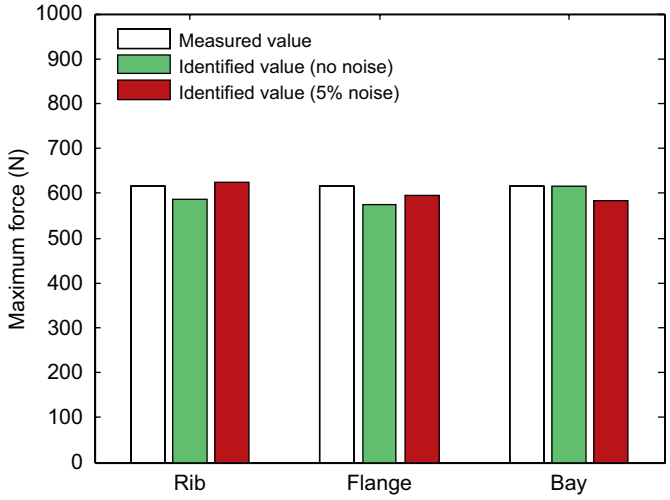

Fig. 10. Comparison of identified and measured maximum forces.

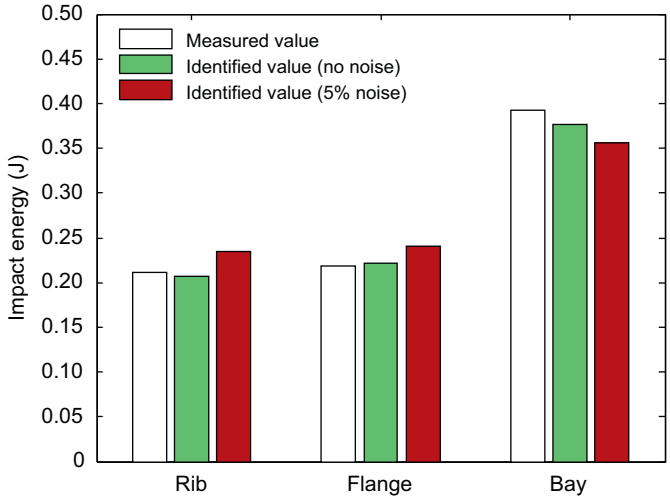

Fig. 11. Comparison of identified and measured impact energies.

The formula for calculating impact energy is [10]:

$$\text{Energy} = \int f(t)\mathrm{d}w \approx \sum_{n=1}^{N_s-1} \frac{[f(n+1)+f(n)]}{2}[w_0(n+1)-w_0(n)] \tag{20}$$

where w_0 is the displacement at the forcing point and can be calculated using the estimated location and force history, N_s is the number of discrete sampling points in the time domain as defined in previous part. The maximum forces for identified and measured impact loads are presented in Fig. 10 and the calculated impact energies for identified and measured impact loads are presented in Fig. 11. In the figures, the identified results without noise are also given. Considering the model deviation and noise effect, the identified maximum forces and impact energies agree quite well with the corresponding measured ones, demonstrating the effectiveness of the proposed impact load identification strategy.

6. Conclusions

This paper proposed a GA-based approach for impact load identification of composite structure. The impact load is represented by a set of parameters, thus the load identification problem in space and time domains is transformed to a parameter identification problem. A forward model characterizes the dynamic response of the structure subject to a known impact force is incorporated. By minimizing the difference between the analytical responses given by the forward model and the measured ones, GA adaptively identify the impact location and time history with its global search capability. This new identification approach has the capability to identify the impact location and reconstruct the impact load history simultaneously.

This method is applied to an impact identification problem for stiffened composite panel. The stiffened composite panel is modeled as an equivalent laminate with varying properties and the forward impact response is obtained by using an assumed modes approach. The effectiveness and applicability of the proposed impact identification strategy is validated by simulation studies. Numerical results show that the proposed GA-based identification approach can not only identify the impact location but also reconstruct the impact load approximately. Though the impact force profile is simplified, the identified maximum impact force and impact energy, which are useful for predicting impact damage in the composite panel, agree the actual ones very well. It only requires the information in time domain, providing a way with simple signal processing. Besides, the μGA employed demonstrates strong capabilities in avoiding premature convergence and accelerating convergence to the near optimal region for this nonlinear multi-modal problem.

Acknowledgements

This research is supported by the National Natural Science Foundation of China under Grant Nos. 50478037 and 10572058, by the Research Foundation for the Doctoral Program of Higher Education under Grant No. 20050287016. Gang Yan would like to appreciate the financial support for Ph.D. dissertation from Nanjing University of Aeronautics and Astronautics under Grant No. BCXJ07-03.

References

[1] F.K. Chang, Structural health monitoring, *Proceedings of the Sixth International Workshop on Structural Health Monitoring*, Stanford, CA, USA, 2007.
[2] L. Gaul, S. Hurlebaus, Identification of the impact location on a plate using wavelets, *Mechanical Systems and Signal Processing* 12 (6) (1998) 783–795.
[3] M. Meo, G. Zumpano, M. Piggott, et al., Impact identification on a sandwich plate from wave propagation responses, *Composite Structures* 71 (3–4) (2005) 302–306.
[4] L. Gual, S. Hurlebaus, Determination of the impact force on a plate by piezoelectric film sensors, *Archive of Applied Mechanics* 69 (9–10) (1999) 691–701.
[5] S.M. Peelamedu, C. Ciocanel, N.G. Naganathan, Impact detection for smart automotive damage mitigation systems, *Smart Materials and Structures* 13 (5) (2004) 990–997.
[6] R.T. Jones, J.S. Sirkis, E.J. Friebele, Detection of impact location and magnitude for isotropic plates using neural networks, *Journal of Intelligent Material Systems and Structures* 8 (1) (1997) 90–99.
[7] D.U. Sung, J.H. Oh, C.G. Kim, et al., Impact monitoring of smart composite laminates using neural network and wavelet analysis, *Journal of Intelligent Material Systems and Structures* 11 (3) (2000) 180–190.
[8] K. Worden, W.J. Staszewski, Impact location and quantification on a composite panel using neural networks and a genetic algorithm, *Strain* 36 (2) (2000) 61–70.
[9] J.R. LeClerc, K. Worden, W.J. Staszewski, et al., Impact detection in an aircraft composite panel—a neural-network approach, *Journal of Sound and Vibration* 299 (3) (2007) 672–682.
[10] K. Choi, F.K. Chang, Identification of impact force and location using distributed sensors, *AIAA Journal* 34 (1) (1996) 136–142.
[11] M. Tracy, F.K. Chang, Identifying impacts in composite plates with piezoelectric strain sensors, part I: theory, *Journal of Intelligent Material Systems and Structures* 9 (11) (1999) 920–928.
[12] R. Seydel, F.K. Chang, Impact identification of stiffened composite panels: I. System development, *Smart Materials and Structures* 10 (1) (2001) 354–369.
[13] S. Matsumoto, H. Fukunaga, N. Hu, Impact force identification of plates using PZT piezoelectric sensors, *Proceedings of the First International Conference on Structural Health Monitoring and Intelligent Infrastructure*, Tokyo, Japan, 2003, pp. 837–845.
[14] N. Hu, H. Fukunaga, S. Matsumoto, et al., An efficient approach for identifying impact force using embedded piezoelectric sensors, *International Journal of Impact Engineering* 34 (7) (2007) 1258–1271.

[15] P.T. Coverley, W.J. Staszewski, Impact damage location in composite structures using optimized sensor triangulation procedure, *Smart Materials and Structures* 12 (5) (2003) 795–803.
[16] J. Haywood, P.T. Coverley, W.J. Staszewski, et al., An automatic impact monitor for a composite panel employing smart sensor technology, *Smart Materials and Structures* 14 (1) (2005) 265–271.
[17] D. Goldberg, *Genetic Algorithms in Search, Optimization and Machine Learning*, Addison-Wesley, Reading, 1989.
[18] H. Holland, *Adaptation in Natural and Artificial System*, MIT Press, Cambridge, MA, 1993.
[19] K. Krishnakumar, Micro-genetic algorithms for stationary and non-stationary function optimization, *Proceedings of SPIE, Intelligent Control and Adaptive Systems*, Philadelphia, PA, USA, 1989, pp. 1196–1228.
[20] D.L. Carroll, Genetic algorithms and optimizing chemical oxygen-iodine lasers, *Developments in Theoretical and Applied Mechanic* 18 (1996) 411–424.
[21] G.L. Giles, Equivalent plate analysis of aircraft wing box structures with general planform geometry, *Journal of Aircraft* 23 (11) (1986) 859–864.
[22] H.P. Lee, T.Y. Ng, Vibration of symmetrically laminated rectangular composite plates reinforced by intermediate stiffeners, *Composite Structure* 29 (4) (1994) 405–413.
[23] H.P. Lee, T.Y. Ng, Effects of torsional and bending restraints of intermediate stiffeners on the free vibration of rectangular plates, *Mechanical Structures and Machines* 23 (1) (1995) 309–320.
[24] R.M. Jose, *Mechanics of Composite Materials*, Scripta Book Co., Washington, 1975.
[25] R. Sydel, Impact Identification of Stiffened Composite Panel, PhD Dissertation, Stanford University, 2000.
[26] J. Dugundji, Simple expressions for higher vibration modes of uniform Euler beams, *AIAA Journal* 26 (8) (1988) 1013–1014.